Cardiovascular Pathology 40 (2019) 32–40

Contents lists available at ScienceDirect

Cardiovascular Pathology

Original Article

Effects of atrial fibrosis induced by mitral regurgitation on atrial electrophysiology and susceptibility to atrial fibrillation in pigs☆

Bo Li [a,1], Fuliang Luo [a,1], Xiaokang Luo [a], Bin Li [a], Lei Qi [a], Dong Zhang [b,*], Yue Tang [a,**]

[a] Animal Experimental Centre, Beijing Key Laboratory of Preclinical Research and Evaluation for Cardiovascular Implant Materials, State Key Laboratory of Cardiovascular Disease, Fuwai Hospital, National Centre for Cardiovascular Disease, Chinese Academy of Medical Sciences and Peking Union Medical College, No. 167 North lishi Road, Xicheng District, Beijing, China
[b] Department of Cardiovascular Surgery, Beijing Jishuitan Hospital, No. 31 Xinjiekou East Street, Xicheng District, Beijing, China

ARTICLE INFO

Article history:
Received 2 November 2018
Received in revised form 22 January 2019
Accepted 23 January 2019

Keywords:
Mitral regurgitation
Animal model
Fibrosis
Atrial fibrillation

ABSTRACT

Background: The mechanism by which atrial fibrosis leads to the production and maintenance of atrial fibrillation (AF) is unclear. Myocardial biopsies, which have often been used in previous studies, are taken from a single site and do not always reflect the overall condition of atrial fibrosis.
Aims: The aim of this study was to investigate the location of fibrosis in the atria induced by mitral regurgitation (MR) and its effect on atrial electrophysiology and vulnerability to AF.
Methods: Nineteen pigs were divided into three groups. The control group (n=6) underwent a sham operation, and the experimental groups underwent an MR induction operation and were observed for 3 (n=7) or 6 (n=6) months. All the animals were tested for vulnerability to AF. Then, the atria were divided into 12 regions: 6 in the left atrium (LA) and 6 in the right atrium (RA). The conduction velocities (CVs) and effective refractory periods (ERPs) in different regions were examined by electroanatomic mapping, and fibrosis in different regions was examined by Masson staining.
Results: With the duration of MR, fibrosis (3.11% ± 0.08% in the control group, 5.85% ± 0.42% in the 3-month group and 8.17% ± 0.23% in the 6-month group, P<.001), vulnerability to AF (0/6 in the control group, 2/7 in the 3-month group and 5/6 in the 6-month group, P<.05) and the effective refractory period (220.1±1.1 ms in the control group, 244.4±1.4 ms in the 3-month group and 289.0±8.9 ms in the 6-month group, P<.001) were increased, while the conduction velocity (1.39±0.16 m/s in the control group, 1.04±0.05 m/s in the 3-month group and 0.89±0.02 m/s in the 6-month group, P<.001) was reduced. These pathophysiological changes were not uniform in different regions of the atria (3.83% ± 0.25% in right atrial fibrosis vs 8.22% ± 0.83% in left atrial fibrosis, P<.001; 5.09% ± 0.34% in the right atrium vs 11.76% ± 0.52% in the left atrium, P<.001). A negative correlation was identified between fibrosis and conduction velocity (P<.001 in the 3-month and 6-month groups), but no correlation was found between fibrosis and the effective refractory period (P=.829 in the 3-month group and P=.093 in the 6-month group). Susceptibility to AF was associated with the dispersion of atrial fibrosis (P=.023).
Conclusions: With the duration of MR, atrial fibrosis increased, and the degree of increase was not uniform among different areas of the atria. The dispersion of atrial fibrosis may contribute to increased susceptibility to AF by influencing the conduction velocity rather than the effective refractory period.

Abbreviations: AF, Atrial fibrillation; MR, Mitral regurgitation; ERP, Effective refractory period; CV, Local conduction velocity; CVF, Collagen volume fraction; SD, Standard deviation; ECG, Electrocardiogram.

☆ Declarations

Ethical approval and consent to participate: All animal procedures were approved by the Animal Welfare Ethics Committee of Fuwai Hospital of Peking Union Medical College, and all experiments were conducted in strict accordance with the National Institutes of Health Guide for the Use of Laboratory Animals.

Competing interests: The authors declare that they have no competing interests to disclose.

Funding: This work was supported by the National Natural Science Foundation of China (Project No: 81370190) and the Innovation Environment and Platform Construction Fund from Beijing Municipal Science and Technology Commission (Project No: Z161100005016014).

Authors' contributions: YT and DZ conceived and designed the experiments; BoL and XL prepared the histology specimens; FL and BinL, who are pathologists specializing in cardiovascular disease, examined the pathological sections; FL and BinL contributed the reagents/materials/analytic tools; BoL and LQ performed the data analysis; BoL and YT wrote the manuscript; and BoL and DZ prepared the figures. All authors reviewed the manuscript.

* Corresponding author. Tel.: +86 17801014009.
** Corresponding author. Tel.: +86 13910713202.
E-mail addresses: xiaoyuanxingyu@126.com (D. Zhang), tangyue@fuwaihospital.org (Y. Tang).

[1] These authors contributed equally to this work.

https://doi.org/10.1016/j.carpath.2019.01.006
1054-8807/

1. Introduction

Atrial fibrosis plays an important role in atrial fibrillation (AF) during both the accumulation of lesions before AF and maintenance after AF induction. Increased atrial fibrosis has been confirmed in patients with increased susceptibility to AF [1], in those with paroxysmal [2], persistent [3], long-standing persistent [4], or valvular AF [5], and in AF animal models induced by burst pacing [6], various operations to increase atrial load combined with burst pacing [7,8], or different AF substrates, including rats and sheep with hypertension [9,10], sheep or dogs with heart failure [11,12], sheep with obesity [13], and rats with diabetes [14].

However, the mechanism of atrial fibrosis that leads to the production and maintenance of AF is unclear. Some studies have provided evidence from post-mortem autopsy findings, analyses of specimens obtained intraoperatively, delayed enhancement-MRI investigations, and electroanatomic mapping studies that some patients with paroxysmal AF have massive fibrosis, whereas some patients with persistent AF have mild fibrosis [15]. In those studies, tissues from a single part of the atrium were used to evaluate atrial fibrosis [2–8], which does not reflect the overall condition of atrial fibrosis. However, the heterogeneity of atrial tissue is thought to be the main characteristic of atrial cardiomyopathy, a gradually accepted matrix of atrial arrhythmias [16], and may lead to heterogeneity of electrical remodeling in the myocardium, which provides the conditions for the occurrence of multiple reentries [17–19]. Overall evaluation of atrial fibrosis can help us to further understand the effects of atrial fibrosis on atrial fibrillation.

In this study, the atria of pigs with mitral regurgitation (MR) were divided into different regions, and the characteristics of fibrosis and electrophysiology in each region were evaluated by histopathology and an electroanatomic mapping system, respectively, to investigate the location of fibrosis in the atria induced by MR and its effect on atrial electrophysiology and vulnerability to AF.

2. Methods

2.1. Animal protocol

Nineteen pigs were divided into three groups. The control group (n=6) underwent a sham operation, and the experimental groups underwent an MR induction operation and were observed for 3 (n=7) or 6 (n=6) months. All the animals underwent an assessment of vulnerability to AF, electroanatomic mapping, and atrial histological analysis after reaching the observation period. All animal procedures were approved by the Animal Welfare Ethics Committee of Fuwai Hospital of Peking Union Medical College, and all experiments were conducted in strict accordance with the National Institutes of Health Guide for the Use of Laboratory Animals.

2.2. Establishment of the MR model

The MR model was established with male miniature pigs provided by the Animal Experimental Center of Fuwai Hospital. The animal models were established by previously described methods (Fig. 1) [20]. Two requirements needed to be met during the operation: the area of the MR beam/left atrium had to be greater than 40%, and the pressure difference in the left atrium before and after the operation had to be greater than 5 mmHg. Anti-heart failure and anti-infection therapy lasting 1–2 weeks after the operation was necessary to cause the model to transition from acute MR to chronic MR.

2.3. AF vulnerability test

The femoral vessels were cannulated, a fixed bent electrode catheter (APT Medical, Inc., Shenzhen) was placed in the coronary sinus for recording, and a 10-pole mapping catheter (APT Medical, Inc., Shenzhen) was placed in the auricula dextra for pacing. The test was carried out as previously described [21]. Rapid pacing lasting 10 s was used to detect vulnerability to AF, with a frequency of 1200 beats per minute, a current of 5 mA and a pulse width of 2.5 ms. Each animal was tested 10 times, and the duration of AF was recorded. The longest duration of AF was considered the final result. AF lasting more than 10 min was considered sustained and was terminated by electrical defibrillation.

2.4. Division of the atria

The atria were partitioned during histopathological examination and electroanatomic mapping (Fig. 2). The right atrium was divided into six regions: the right atrial auricle, tricuspid isthmus, anterior and posterior walls of the right atrium, and superior and inferior entrances of the vena cava. The tricuspid isthmus was defined as the area between the tricuspid valve and the inferior vena cava. The posterior wall of the right atrium was defined as the area surrounded by the cristae terminalis and the posterior edge of the atrial septum. The anterior wall of right the atrium was defined as the adjacent area prior to the cristae terminalis. The entrance of the vena cava was defined as the transitional area of the vena cava and atrium. The left atrium was divided into six regions: the left atrial auricle, atrial septum, left atrial posterior wall, top of the left atrium, ostia venarum pulmonalium, and mitral isthmus. The mitral isthmus was defined as the area between the lower edge of the lower pulmonary vein and the mitral annulus. The posterior wall of the left atrium was defined as the central area surrounded by the pulmonary vein orifice. The top of the left atrium was defined as the area above the superior edge of the superior pulmonary vein. The atrial septum was defined as the common wall of the left and right atria. The pulmonary vein orifice was defined as the transitional areas of pulmonary veins and the atrium.

2.5. Electroanatomic mapping

Left atrial activation mapping was performed during sinus rhythm using an electroanatomic mapping system (Hongtong Industry, Shanghai) and a pulmonary venous annular mapping catheter (APT Medical, Inc., Shenzhen). When the electrode catheter is dragged along the

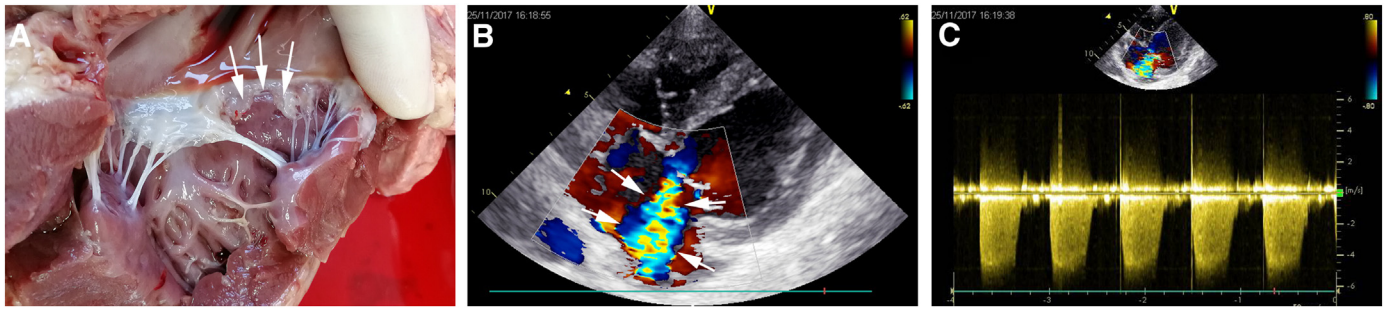

Fig. 1. Mitral valve and ultrasound imaging. (A) The white arrows indicate the mitral valve leaflet with a broken tendon, which includes the P2 and P3 areas. (B) The apical four-chamber view showing blood flowing through the mitral valve and back into the left atrium. (C) Continuous-wave Doppler at the level of the mitral valve showing holosystolic regurgitant flow.

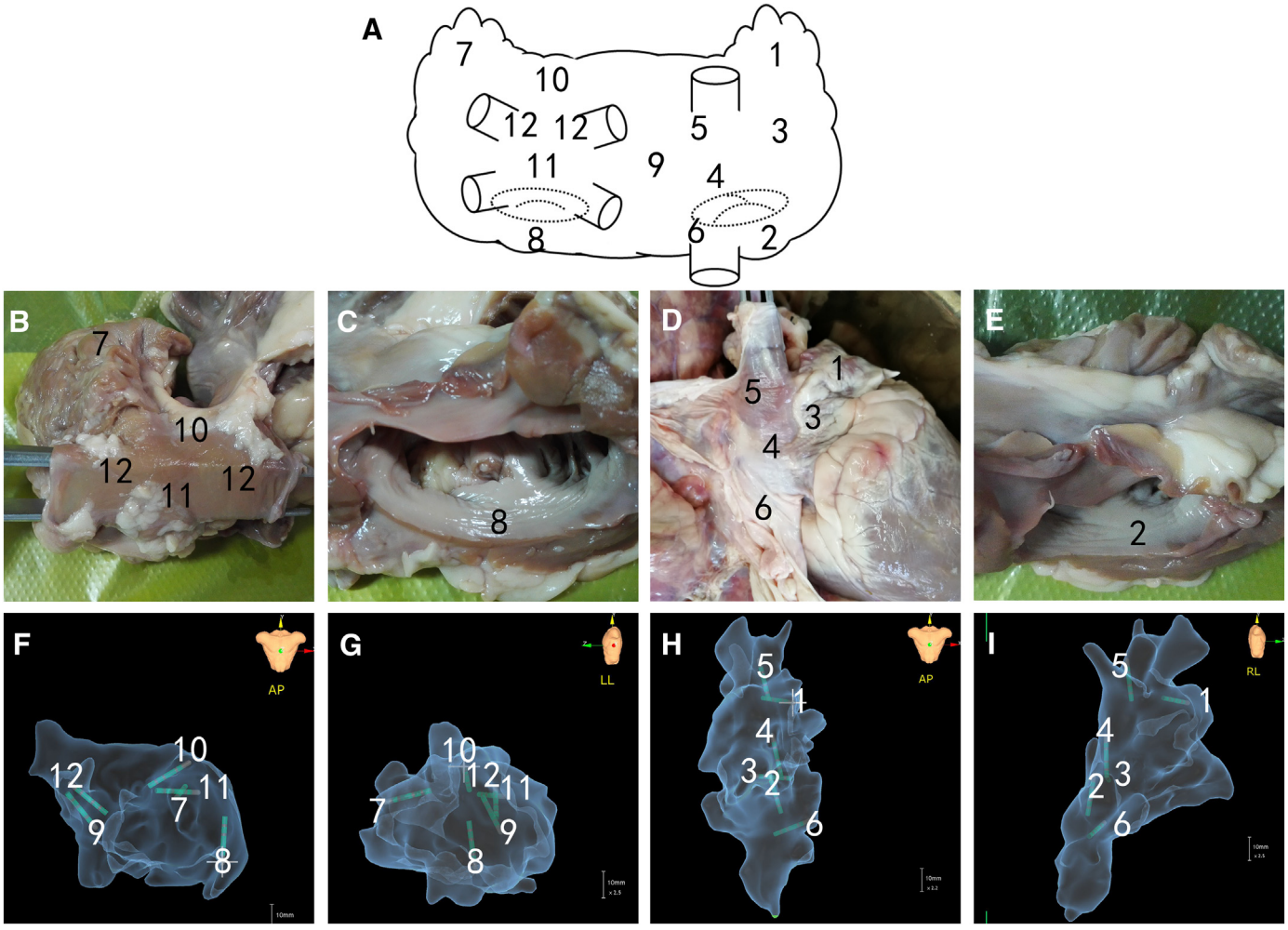

Fig. 2. Division and nomenclature of the atria. A is a diagrammatic sketch of the atria; B, C, D and E are actual photographs of the atria; F, G, H and I are 3D electroanatomic mapping images. The right atrium was divided into six regions: 1. right atrial auricle, 2. tricuspid isthmus, 3. anterior wall of the right atrium, 4. posterior wall of the right atrium, 5. superior vena cava entrance, and 6. inferior vena cava entrance. The left atrium was divided into six regions: 7. left atrial auricle, 8. mitral isthmus 9. atrial septum, 10. top of the left atrium, 11. left atrial posterior wall, and 12. ostia venarum pulmonalium.

endocardium, the system automatically stores each endocardial contact point. The heart cavity was mapped automatically and displayed on a display screen in three-dimensional form (Fig. 3). Some images that were considered abnormal by the operator were removed by an engineer.

2.6. Effective refractory period (ERP) test

ERPs were measured with the S1S2 method at the twelve locations of the atrium. Four-times the diastolic threshold was used for the test,

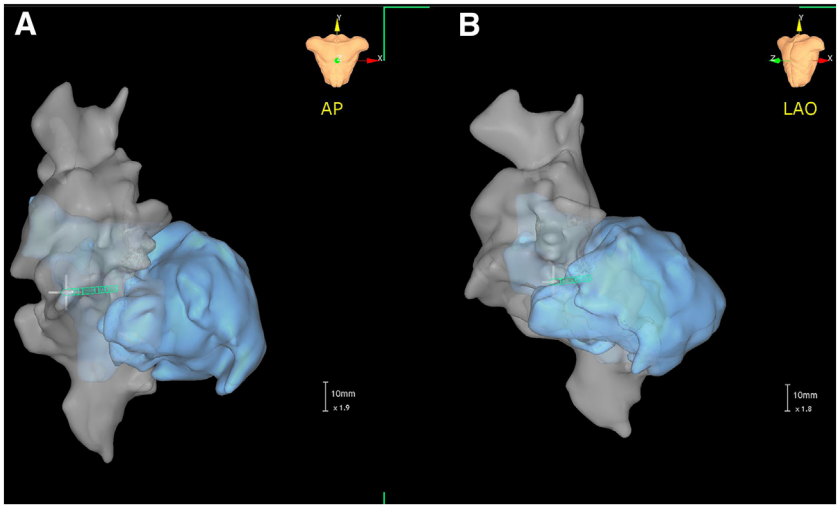

Fig. 3. Atrial structure by electroanatomic mapping. The right atrium is gray, and the left atrium is blue and is shown in a positive posterior position (A) and a left anterior oblique position (B).

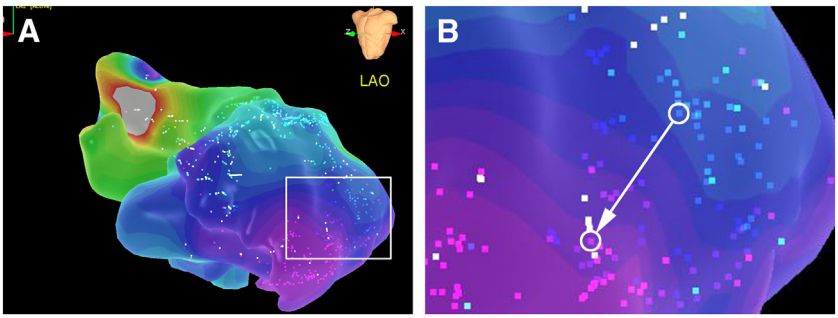

Fig. 4. Calculation of CV. A color-coded atrial activation sequence diagram was created, with red indicating the earliest active region and purple indicating the last active region. B. The conduction velocity between the two measured points was defined as the distance between the two points divided by the difference in activation time.

and S2 was decreased in 5-ms steps after 8-beat drive trains with basic cycle lengths of 450 ms. The ERP was defined as the first S1-S2 interval that did not depolarize the atrium.

2.7. Local conduction velocity (CV)

The CVs were measured according to methods reported in previous literature [22]. A color-coded atrial activation sequence diagram was created, with red indicating the earliest activation area and purple indicating the latest activation area. The CV between the two measured points was defined as the distance between the two points divided by the difference in activation time (Fig. 4).

2.8. Histological analyses

Atrial tissue was removed immediately after the animals were euthanized, and the epicardial connective tissue was removed to avoid overestimating fibrosis. The atrial tissue was cut into small pieces, approximately 1.0×0.5 cm in size, and fixed in 10% formalin for 48 h. The tissue was rinsed with running water for 3 h to remove any residual fixative. Dehydration, clearing and paraffin infiltration of the tissues were performed with a vacuum tissue processor (Leica ASP200). Embedding was performed with a paraffin embedding station (Leica EG1150H). Sectioning was performed with a manual rotary microtome (Leica RM2235) with a thickness of 4 μm. Pathological sections were produced with a water bath and slice baking machine (Leica HI1220). Masson staining was performed with a trichrome staining (Masson) kit (Sigma Inc., USA) to assess fibrosis. All operations were performed according to the manual included in the Masson kit: Stain in working Weigert's iron hematoxylin solution for 5 min. Wash in running tap water for 5 min. Rinse in deionized water. Stain in Biebrich scarlet-acid Fuchsin for 5 min. Rinse in deionized water. Place slides in working phosphotungstic/phosphomolybdic acid solution for 5 min. Place slides in aniline blue solution for 5 min. Place slides in 1% acetic acid for 2 min. Discard solution. Rinse slides, dehydrate with alcohol, clear in xylene and mount. The coverslips used were Consul coverslips (Leica CV5030). Collagen stained blue, and myocardial cells stained red. The pathological sections were photographed with a microscope (Zeiss Axio Scan.Z1). Images were stored and used for semi-quantitative analysis of the extent of fibrosis with Image-Pro Plus 6.0 (GelDoc2000, Bio-Rad). The blue area was automatically measured and could be manually corrected if necessary such that the blue area in the field of vision could be calculated correctly. The collagen volume fraction was calculated as follows: collagen volume fraction (CVF, %) = (total area of collagen/total area of the image) × 100%. For each specimen, 10 fields were randomly selected, and the average value was taken as the final result.

2.9. Statistical analysis

Continuous variables (fibrosis, CV, ERP and AF duration) are expressed as the mean ± standard deviation (SD), and categorical data (vulnerability to AF) are expressed as numbers. Comparisons of quantitative data between two groups were tested using t-tests. Comparisons of quantitative data between multiple groups were tested with one-way ANOVA and the LSD test. Categorical data between groups were compared using the chi-square test. The correlation between two continuous variables was analyzed by measuring Pearson's correlation coefficient (r). Multiple linear regression was used to assess the association between vulnerability to AF and atrial fibrosis. Separate models were developed using the duration of atrial fibrillation as the outcome variable. The independent variables were the standard deviation of fibrosis and the mean of fibrosis. $P<.05$ was considered statistically significant. The software SPSS 24.0 was used for statistical analysis.

3. Results

3.1. Vulnerability to AF

The experimental animals in each group were randomly examined with electrocardiograms (ECGs) before and after the operation, and no

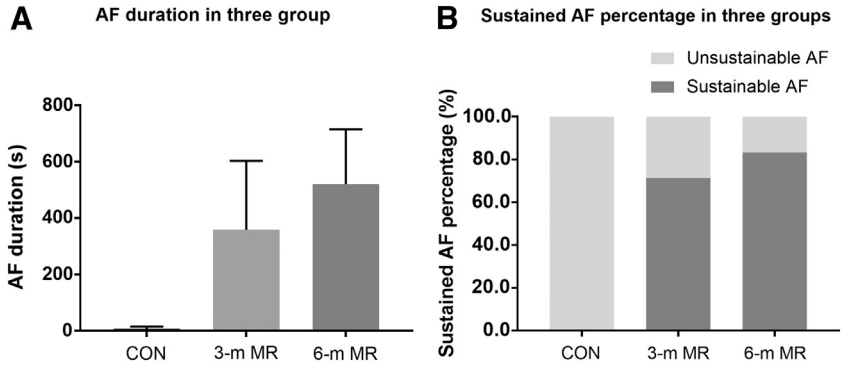

Fig. 5. Results of the AF vulnerability test. The mean duration of atrial fibrillation (A) and the percentage of sustained AF (B) in the three groups.

spontaneous AF was noted. All the animals were tested for vulnerability to AF. Sustained AF (>10 min) was not observed in any of the 6 control pigs, while sustained AF was inducible in 2 of 7 pigs in the 3-month group and 5 of 6 pigs in the 6-month group (χ^2, $P<.05$) (Fig. 5). The average longest duration of an AF episode was 6.7±8.4 s in the control group, 287.0±231.4 s in the 3-month group and 520.0±195.1 s in the 6-month group.

3.2. Histological analyses

The average values of fibrosis in the 12 sites of the atria were defined as the mean of atrial fibrosis, and the average values of fibrosis in the 6 sites in right and left atria were defined as the mean value of right fibrosis and the mean value of left atrial fibrosis, respectively. Similar calculations were performed for the CV and ERP.

3.2.1. Fibrosis increased with the duration of MR

The mean values of atrial fibrosis increased with the duration of MR and were 3.11% ± 0.08% in the control group, 5.85% ± 0.42% in the 3-month group and 8.17% ± 0.23% in the 6-month group ($P<.001$). A separate comparison of the mean values of left atrial and right atrial fibrosis also showed similar results. The mean values of right atrial fibrosis were 3.11% ± 0.18% in the control group, 3.83% ± 0.25% in the 3-month group and 5.09% ± 0.34% in the 6-month group ($P<.001$), while the mean values of left atrial fibrosis were 3.11% ± 0.24%, 8.22% ± 0.83% and 11.76% ± 0.52%, in the control, 3-month and 6-month groups, respectively ($P<.001$).

3.2.2. Fibrosis in different parts of the atrium was inconsistent

No difference was observed between the mean values of left and right atrial fibrosis in the control group (3.11% ± 0.18% and 3.11% ± 0.24%, respectively, $P=.960$). The mean value of left atrial fibrosis was higher than that of right atrial fibrosis in the 3-month (3.83% ± 0.25% and 8.22% ± 0.83%, respectively, $P<.001$) and 6-month groups (5.09% ± 0.34% and 11.76% ± 0.52%, respectively, $P<.001$). Among the three groups, no difference was observed in fibrosis between the six different parts of the right atrium ($P=.669$ in the control group, $P=.848$ in the 3-month group, and $P=.458$ in the 6-month group). A significant difference in fibrosis was observed between the six different parts of the left atrium in the 3-month ($P<.001$) and 6-month groups ($P<.001$), but no difference was found in the control group ($P=.846$) (Figs. 6, 7A and 8).

3.3. Local CV

3.3.1. Atrial CV decreased with the duration of MR

The mean atrial CVs decreased with the duration of MR and were 1.39±0.16 m/s in the control group, 1.04±0.05 m/s in the 3-month group and 0.89±0.02 m/s in the 6-month group ($P<.001$). A separate comparison of the left atrium and the right atrium also showed similar results. The mean right atrial CVs were 1.41±0.14 m/s in the control group, 1.20±0.03 m/s in the 3-month group and 1.13±0.03 m/s in the 6-month group ($P<.001$), while the mean left atrial CVs were 1.36± 0.22 m/s, 0.86±0.08 m/s and 0.62±0.02 m/s in the control, 3-month and 6-month groups, respectively ($P<.001$).

3.3.2. Atrial CVs in different parts of the atria were inconsistent

No difference was observed between the mean left and right atrial CVs in the control group (1.45±0.10 and 1.44±0.08, respectively, $P=.860$). The mean left atrial CV was lower than the right atrial CV in the 3-month (0.86±0.07 and 1.20±0.32, respectively, $P<.001$) and 6-month groups (0.62±0.02 and 1.13±0.03, respectively, $P<.001$). No difference was observed in the CV in the six different parts of the right atrium ($P=.705$ in the control group; $P=.646$ in the 3-month group; and $P=.066$ in the 6-month group). A difference in the CV was found between the six different parts of the left atrium in the 3-month ($P<.001$) and 6-month groups ($P<.001$), but no difference was found in the control group ($P=.543$) (Fig. 7B).

3.4. ERP

3.4.1. ERP increased with the duration of MR

The mean ERPs increased with the duration of MR and were 220.1± 1.1 ms in the control group, 244.4±1.4 ms in the 3-month group and

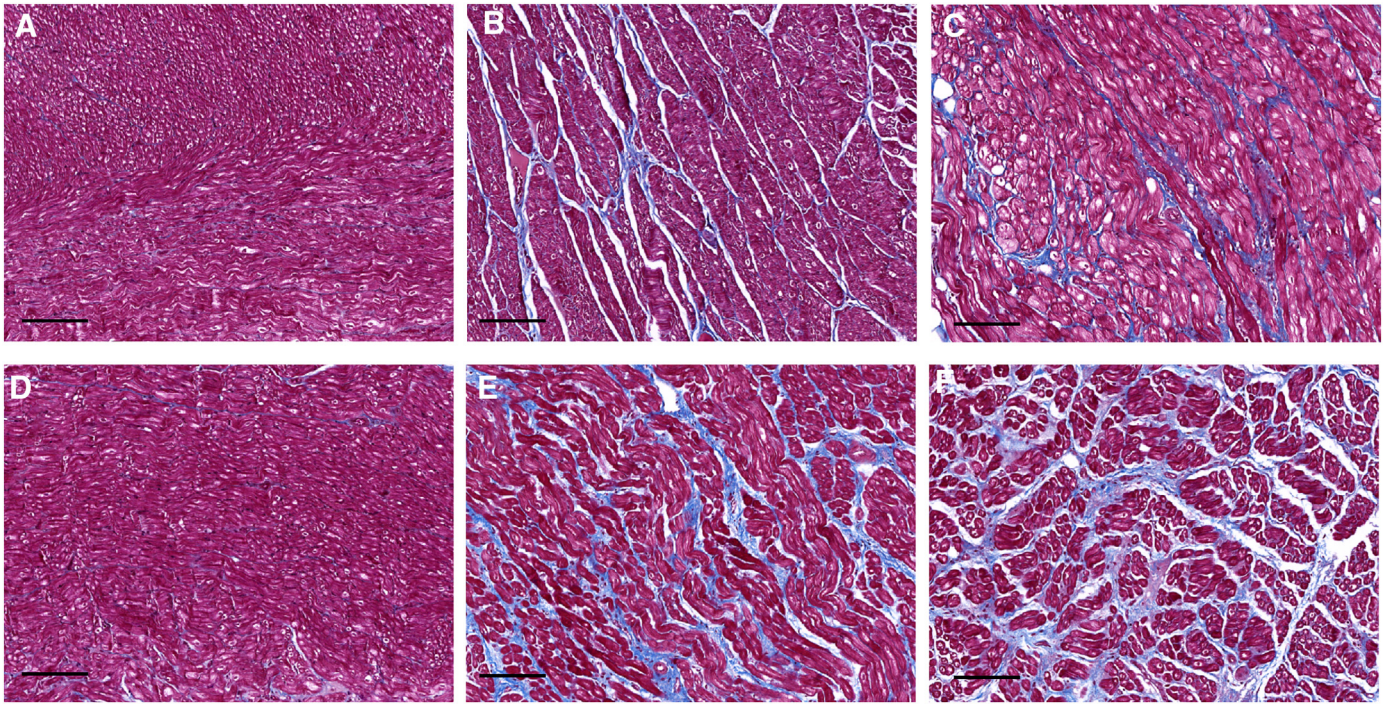

Fig. 6. Masson staining of the left atrial auricle and left atrial posterior wall Masson staining of left atrial auricle in the control group (A), 3-month group (B) and 6-month group (C); Masson staining of the left atrial posterior wall in the control group (D), 3-month group (E) and 6-month group (F) (bar=100 μm).

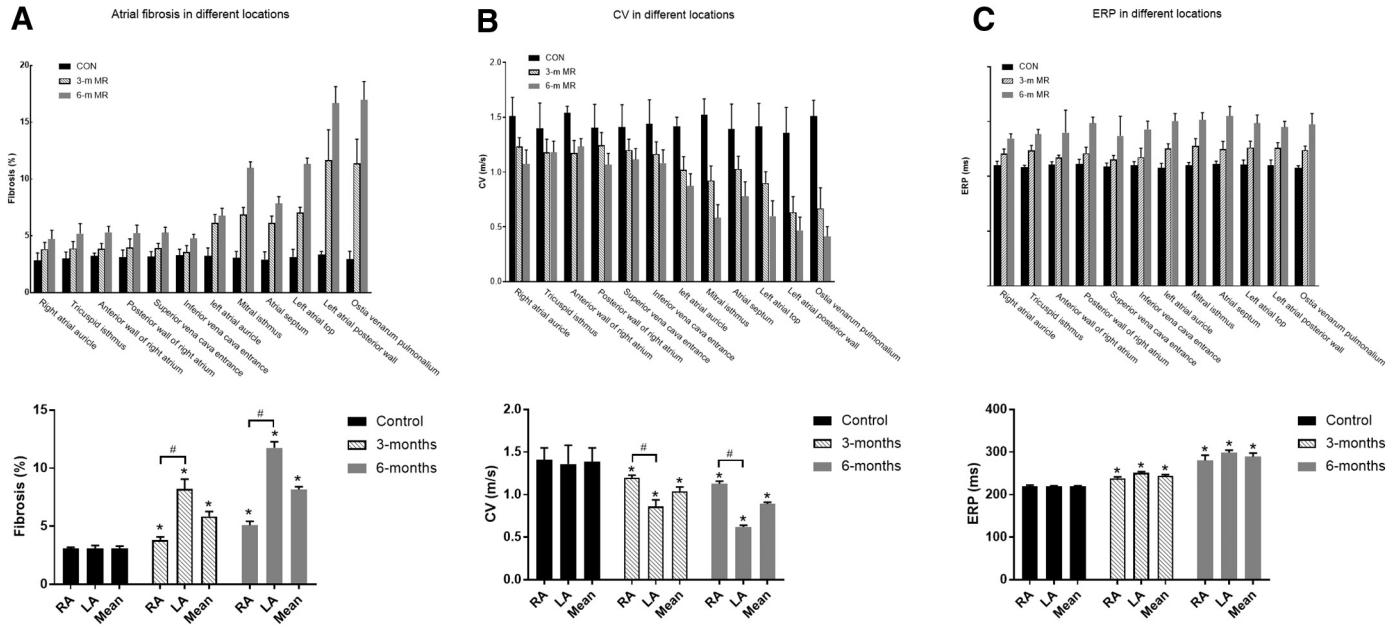

Fig. 7. Fibrosis (A), CV (B) and ERP (C) in different parts of the atria in the three groups of experimental animals.

289.0±8.9 ms in the 6-month group (P<.001). A separate comparison of the ERPs of the left atrium and the right atrium also showed similar results. The mean ERPs of the right atrium were 220.2±2.3 ms in the control group, 238.6±3.1 ms in the 3-month group and 280.5±12.4 ms in the 6-month group (*P*<.001), while the mean ERPs of left atrium were 219.5±1.8, 251.4±2.9 and 299.3±5.3 in the control, 3-month and 6-month groups, respectively (*P*<.001).

3.4.2. Atrial CVs in different parts of the atrium were inconsistent

No difference was observed between the left and right atrial ERPs in the control group (220.2±2.3 ms and 219.5±1.8 ms, *P*=.670). The left atrial ERP was longer than the right atrial ERP in the 3-month (238.6± 3.1 ms and 251.4±2.9 ms, *P*=.001) and 6-month groups (299.3± 5.3 ms and 280.5±12.4 ms, *P*=.003) (Fig. 7C).

3.5. Vulnerability to AF was associated with the distribution of left atrial fibrosis

The distribution of fibrosis in different parts of the left atrium increased with the duration of MR. In the 6-month group, the SD and coefficient of variation of left atrial fibrosis were 4.30% and 0.37, respectively, and in 3-month group, these values were 2.61% and 0.32, respectively, while the SD and coefficient of variation were only 0.16% and 0.05, respectively, in the control group. Multiple linear regression models showed that the standard deviation rather than the mean value of fibrosis was associated with the duration of atrial fibrillation (Table 1).

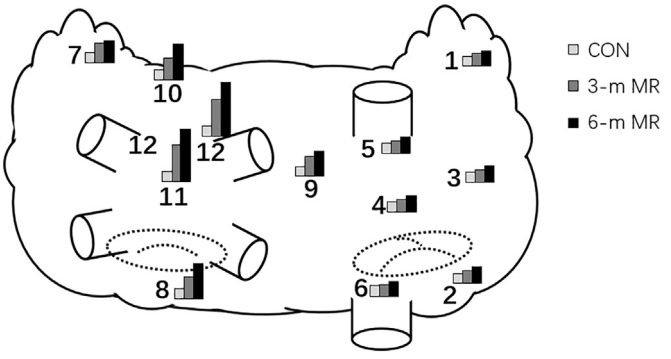

Fig. 8. Fibrosis in different parts of the atria in the three groups of experimental animals. The height of the column represents the degree of fibrosis.

3.6. Relationship among fibrosis, ERP, and CV

Data from different locations of the left atrium in the MR groups were used for a correlation analysis. A negative correlation was identified between fibrosis and CV in the 3-month group (Pearson correlation coefficient: -0.701, *P*<.001) and the 6-month group (Pearson correlation coefficient: -0.830, *P*<.001). No correlation was found between fibrosis and the ERP in the 3-month group (Pearson correlation: -0.034, *P*= .829) or the 6-month group (Pearson correlation: -0.284, *P*=.093) (Fig. 9).

4. Discussion

The major finding of this study is that varying degrees of atrial fibrosis occur in different parts of the atria during MR, which may affect vulnerability to AF by influencing atrial CV. We can see from this study that fibrosis in the left atrium is more serious than fibrosis in the right atrium. In the left atrium, the posterior wall and pulmonary vein orifice develop the most severe fibrosis, followed by the top of the left atrium and the mitral isthmus, and then the atrial appendage and the atrial septum. The vulnerability to AF increased with increases in the mean value of atrial fibrosis. Atrial CV decreased with the duration of MR and was negatively correlated with atrial fibrosis. The ERP of the atria was prolonged with the duration of MR but was not associated with atrial fibrosis.

During MR, the formation and redistribution of connective tissue fibers modulate the geometric structure of the myocardium to adapt to new pathophysiological functional conditions and to prevent or minimize the effects of new mechanical, chemical and electrical stimuli

Table 1
Multiple linear regression models showing that the standard deviation rather than the mean value of fibrosis is associated with the duration of atrial fibrillation

Independent variables	β	Standard error	Standardized β	*P*
Average of fibrosis	−49.972	64.103	−0.378	.447
Standard deviation of fibrosis	559.255	221.967	1.250	.023

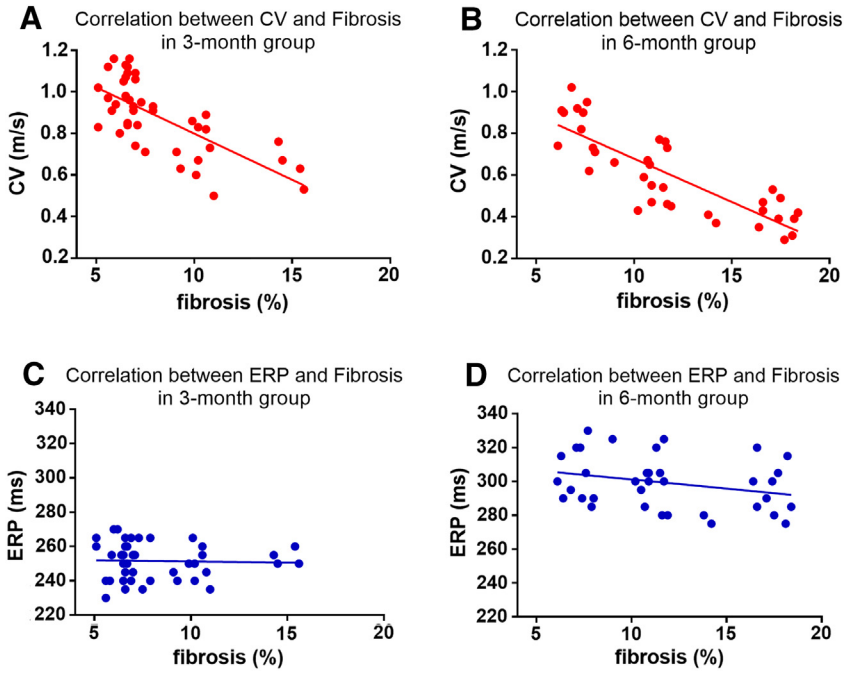

Fig. 9. The relationship between fibrosis and CV in the 3-month (A) and 6-month groups (B); The relationship between fibrosis and ERP in the 3-month (C) and 6-month groups (D).

[23]. This adaptation process involves changes in cellular components as well as changes in the extracellular matrix [24]. This myocardial remodeling has been considered to be atrial cardiomyopathy, which is defined as "any complex of structural, architectural, contractile or electrophysiological changes affecting the atria with the potential to produce clinically relevant manifestations" and is divided into four categories according to changes in cardiomyocytes and fibrosis. Valvular atrial cardiomyopathy is classified as category III, remodeling combined with cardiomyocyte pathology and fibrosis [16]. The reasons for atrial fibrosis due to MR may be as follows: Increased left atrial strain induced by MR promotes fibrosis, and the uneven strain of the left atrium caused by left atrial blood turbulence [25] may be the cause of the heterogeneity of atrial fibrosis. Increased hormones during MR, such as angiotensin [26] and endothelin-1 [27], can also promote myocardial fibrosis. Uneven distribution of receptors in the atrium may be another cause of the heterogeneity of atrial fibrosis.

AF is associated with structural and electrical remodeling of the atria. The occurrence and progression of atrial fibrosis are hallmarks of structural remodeling, and atrial fibrosis is considered the substrate for AF maintenance. Advanced atrial fibrosis is associated with more frequent paroxysms of AF, transformation of AF into a permanent type, and reduced effectiveness of antiarrhythmic drug [28], ablation [29] or maze operation [5] therapy. These results have also been confirmed in this experiment, and prolongation of the AF duration is related to the mean value of atrial fibrosis and the mean values of right and left atrial fibrosis. However, some previous studies have found that some patients with paroxysmal AF have massive fibrosis, while some patients with persistent AF show mild fibrosis [15]. This outcome may be due to two reasons: (1) In previous studies, atrial samples were often taken from a single site, which did not represent the overall fibrotic state of the atria. In this study, increased AF vulnerability was associated with the mean value of atrial fibrosis rather than fibrosis of a single site. (2) Atrial fibrosis is dependent not only on severity but also on another dimension that affects AF. In this experiment, one animal with a higher degree of fibrosis in the 6-month group showed a negative result on the AF vulnerability test, while two animals with a lesser degree of fibrosis in the three-month group showed a positive result on the AF vulnerability test. The heterogeneity of atrial fibrosis seems to be associated with AF. This view is proved by the fact that the sustained AF pigs had greater SDs and coefficients of variation of fibrosis in different parts compared to the non-sustained AF pigs in the MR groups.

Collagen deposition in the extracellular stroma of cardiomyocytes results in increased myocyte-myocyte distances and physically blocks atrial conduction, which can cause decreased CV and regional conduction block [30]. Induction of an activation delay, which is caused by propagation of the activation front around inexcitable barriers of collagen, can be observed in atrial tissue in patients with AF [31]. Other investigators have shown that sites of increased fibrosis are often involved in the generation of a unidirectional conduction block [32]. Factors other than the lack of conduction by collagen fibrils may explain the decreased CV in fibrotic regions. Some evidence suggests that myocytes may form electrical connections with fibroblasts through gap junctions, while these cells have different electrophysiological properties compared to the surrounding cardiomyocytes. Fibroblasts are essentially nonexcitable cells but can transfer currents between cardiomyocytes via connexins in vitro. An uneven distribution of fibroblasts may result in heterogeneous current conduction [33]. Three-dimensional computational models based on patient-specific atrial geometry revealed proliferation of myofibroblasts and that their electrical interaction with cardiomyocytes was sufficient for re-entry formation, even in the absence of fibrosis [34]. These data are compatible with our observation that interstitial fibrosis leads to discontinuous propagation and spatial dispersion of conduction, creating a potential substrate for re-entry. During rapid pacing, the atria show high anisotropy and activation delays, which may result in heterogeneous conduction, such as the occurrence of a unidirectional conduction block and re-entry, facilitating both the induction and maintenance of AF. Thus, radiofrequency or other thermal ablation and surgical sectioning may address atrial fibrillation by blocking the path of re-entry at the edges of different areas with different fibrosis levels [35,36].

The ERPs in different parts of the atria were detected in this study. The results showed that the mean ERP was prolonged during MR, and this condition was aggravated by the duration of MR. This finding is consistent with those of previous animal model studies [21,37] and clinical observatories [38] in which an increase in the atrial ERP was considered to be associated with atrial dilation. However, other studies have also shown no change [39] or a decrease [40,41] in the atrial ERP during atrial dilation. A decrease in the atrial ERP is considered to promote

the occurrence of re-entry arrhythmias, whereas prolongation of the atrial ERP is often considered to be a protective mechanism against arrhythmias. In this study, as MR continued, the ERP not only became prolonged but its dispersion also increased, which fits with another view that dispersion of the ERP is an important cause of AF [42,43]. Prolongation of the atrial ERP and the increase in dispersion may be induced by other causes, such as inflammation [44] and changes in the autonomic nervous system [45] and ion channels [46], which are not affected by fibrosis or synchronized with the progression of fibrosis.

The relationship between the distribution of fibrosis and atrial fibrillation has many prospective clinical applications. The distribution of fibrosis can be used as a predictor of atrial fibrillation; for example, MR patients at a high risk of atrial fibrillation may benefit from more aggressive surgical treatment [47]. With the generalization of ablation treatment for atrial fibrillation, limited overall success rates and a frequent need for re-ablations are problems that currently concern doctors. A better understanding of an arrhythmia's substrate will provide more ideas to improve ablation protocols [48]. In addition, the development of various detection technologies has minimized the difficulty of detecting atrial fibrosis. A variety of methods, such as echocardiography [49], cardiac magnetic resonance imaging [50], and three-dimensional electroanatomic mapping [51], can be used to detect fibrosis, which allows us to understand atrial fibrosis in patients with AF without myocardial biopsies and to conduct more studies on the relationship between atrial fibrillation and the distribution of fibrosis.

The increased susceptibility to atrial fibrillation caused by MR is due to multiple causes and not simply atrial fibrosis. Chronic atrial dilatation is thought to be another cause of atrial fibrillation during MR. Almost all of the diseases associated with a high incidence of atrial fibrillation are associated with enlargement of the left atrium, such as aortic stenosis [48], heart failure [52], and mitral stenosis [53]. In these AF models, with either rapid pacing [54] or heart failure [55], the size of the LA increases. Studies have shown that dilation of the left atrium leads to shortening of the effective refractory period of the atrium, which is thought to be the cause of atrial fibrillation.

5. Limitations

This study has the following limitations: (1) All experimental animals used in this study were juvenile pigs. The effect of age on myocardial fibrosis or AF susceptibility was not evaluated in this study but may be of critical importance in humans. (2) In this study, MR in experimental animals was caused by rupturing the chordae tendineae of the posterior mitral valve leaflet; however, human MR occurs through different mechanisms. (3) Myocardial fibrosis is more likely to develop in pigs [56], and myocardial fibrosis occurs by different processes in humans and pigs during MR. Further study of human myocardial tissue is necessary. (4) The atrial segmentation in this study was bulky, and the degree of fibrosis in the same area may not have been consistent. We only calculated the average fibrosis of an area to represent the degree of fibrosis in the region. More detailed segmentation could more realistically reflect the distribution of fibrosis. (5) Electroanatomic mapping and pathological anatomy can only reflect regional relativity rather than point-to-point relativity, which inevitably leads to spatial differences between electrophysiological data and pathological data.

6. Conclusion

With the duration of MR, atrial fibrosis increased, and the degree of increase was not uniform in different areas of the atria. Fibrosis in the left atrium is more serious than fibrosis in the right atrium. In the left atrium, the posterior wall and pulmonary vein orifice had the most severe fibrosis, followed by the top of the left atrium and the mitral isthmus, and then the atrial appendage and atrial septum. The distribution of atrial fibrosis in different locations of the atrium may contribute to increased vulnerability to atrial fibrillation. Atrial fibrosis may achieve this effect by influencing the conduction velocity rather than the effective refractory period.

Acknowledgements

We thank all the staff of Beijing Key Laboratory of Preclinical Research and Evaluation for Cardiovascular Implant Materials who contributed to the experiment.

References

[1] Pandit SV, Anumonwo J, Jalife J. Atrial fibrillation susceptibility in obesity: an excess adiposity and fibrosis complicity. Circ Res 2016;118:1468–71.
[2] Canpolat U, Aytemir K, Hazirolan T, Özer N, Oto A. Relationship between vitamin D level and left atrial fibrosis in patients with lone paroxysmal atrial fibrillation undergoing cryoballoon-based catheter ablation. J Cardiol 2017;69(1):16–23.
[3] Liu Y, Niu XH, Yin X, et al. Elevated circulating Fibrocytes is a marker of left atrial fibrosis and recurrence of persistent atrial fibrillation. J Am Heart Assoc 2018;7(6).
[4] Li Z, Wang Z, Yin Z, et al. Gender differences in fibrosis remodeling in patients with long-standing persistent atrial fibrillation. Oncotarget 2017;8(32):53714–29.
[5] Kainuma S, Masai T, Yoshitatsu M, et al. Advanced left-atrial fibrosis is associated with unsuccessful maze operation for valvular atrial fibrillation. Eur J Cardiothorac Surg 2011;40(1):61–9.
[6] Kiryu M, Niwano S, Niwano H, et al. Angiotensin II-mediated up-regulation of connective tissue growth factor promotes atrial tissue fibrosis in the canine atrial fibrillation model. Europace 2012;14(8):1206–14.
[7] Tang M, Zhang S, Sun Q, Huang C. Alterations in electrophysiology and tissue structure of the left atrial posterior wall in a canine model of atrial fibrillation caused by chronic atrial dilatation. Circ J 2007;71(10):1636–42.
[8] Remes J, van Brakel TJ, Bolotin G, et al. Persistent atrial fibrillation in a goat model of chronic left atrial overload. J Thorac Cardiovasc Surg 2008;136(4):1005–11.
[9] Lau DH, Mackenzie L, Kelly DJ, et al. Short-term hypertension is associated with the development of atrial fibrillation substrate: a study in an ovine hypertensive model. Heart Rhythm 2010;7(3):396–404.
[10] Lau DH, Shipp NJ, Kelly DJ, et al. Atrial arrhythmia in ageing spontaneously hypertensive rats: unraveling the substrate in hypertension and ageing. PLoS One 2013;8(8):e72416.
[11] Lau DH, Psaltis PJ, Mackenzie L, et al. Atrial remodeling in an ovine model of anthracycline-induced nonischemic cardiomyopathy: remodeling of the same sort. J Cardiovasc Electrophysiol 2011;22(2):175–82.
[12] Li D, Fareh S, Leung TK, Nattel S. Promotion of atrial fibrillation by heart failure in dogs: atrial remodeling of a different sort. Circulation 1999;100(1):87–95.
[13] Mahajan R, Lau DH, Brooks AG, et al. Electrophysiological, Electroanatomical, and structural remodeling of the atria as consequences of sustained obesity. J Am Coll Cardiol 2015;66(1):1–11.
[14] Linz D, Hohl M, Dhein S, et al. Cathepsin a mediates susceptibility to atrial tachyarrhythmia and impairment of atrial emptying function in Zucker diabetic fatty rats. Cardiovasc Res 2016;110(3):371–80.
[15] Kottkamp H. Human atrial fibrillation substrate: towards a specific fibrotic atrial cardiomyopathy. Eur Heart J 2013;34(35):2731–8.
[16] Goette A, Kalman JM, Aguinaga L, et al. EHRA/HRS/APHRS/SOLAECE expert consensus on atrial cardiomyopathies: definition, characterisation, and clinical implication. J Arrhythm 2016;32(4):247–78.
[17] Spach MS, Dolber PC, Heidlage JF. Interaction of inhomogeneities of repolarization with anisotropic propagation in dog atria. A mechanism for both preventing and initiating reentry. Circ Res 1989;65(6):1612–31.
[18] Varela M, Colman MA, Hancox JC, Aslanidi OV. Atrial heterogeneity generates re-entrant substrate during atrial fibrillation and anti-arrhythmic drug action: mechanistic insights from canine atrial models. PLoS Comput Biol 2016;12(12):e1005245.
[19] Aslanidi OV, Colman MA, Varela M, et al. Heterogeneous and anisotropic integrative model of pulmonary veins: computational study of arrhythmogenic substrate for atrial fibrillation. Interface Focus 2013;3(2):20120069.
[20] Li B, Cui Y, Zhang D, et al. The characteristics of a porcine mitral regurgitation model. Exp Anim 2018.
[21] Verheule S, Wilson E, Everett T, Shanbhag S, Golden C, Olgin J. Alterations in atrial electrophysiology and tissue structure in a canine model of chronic atrial dilatation due to mitral regurgitation. Circulation 2003;107(20):2615–22.
[22] Fukumoto K, Habibi M, Ipek EG, et al. Association of Left Atrial Local Conduction Velocity with Late Gadolinium Enhancement on cardiac magnetic resonance in patients with atrial fibrillation. Circ Arrhythm Electrophysiol 2016;9(3):e002897.
[23] Dzeshka MS, Lip GY, Snezhitskiy V, Shantsila E. Cardiac fibrosis in patients with atrial fibrillation: Mechanisms and Clinical Implications. J Am Coll Cardiol 2015;66(8):943–59.
[24] Murtha LA, Schuliga MJ, Mabotuwana NS, et al. The processes and mechanisms of cardiac and pulmonary fibrosis. Front Physiol 2017;8:777.
[25] Gnyawali SC, Roy S, Driggs J, Khanna S, Ryan T, Sen CK. High-frequency high-resolution echocardiography: first evidence on non-invasive repeated measure of myocardial strain, contractility, and mitral regurgitation in the ischemia-reperfused murine heart. J Vis Exp 2010(41).
[26] Liu WH, Fang YN, Wu CC, Chen MC, Chang JP, Lin YS, et al. Differential gene expression profile of renin-angiotensin system in the left atrium in mitral regurgitation patients. Dis Markers 2018;2018:6924608.

[27] Mayyas F, Niebauer M, Zurick A, Barnard J, Gillinov AM, Chung MK, et al. Association of left atrial endothelin-1 with atrial rhythm, size, and fibrosis in patients with structural heart disease. Circ Arrhythm Electrophysiol 2010;3(4):369–79.
[28] Spragg D. Left atrial fibrosis: role in atrial fibrillation pathophysiology and treatment outcomes. J Atr Fibrillation 2013;5(6):810.
[29] Selvendran S, Aggarwal N, Li J, Tse G, Vassiliou VS. The role of myocardial fibrosis in determining the success rate of ablation for the treatment of atrial fibrillation. Minerva Cardioangiol 2017;65(4):420–6.
[30] Verheule S, Tuyls E, Gharaviri A, et al. Loss of continuity in the thin epicardial layer because of endomysial fibrosis increases the complexity of atrial fibrillatory conduction. Circ Arrhythm Electrophysiol 2013;6(1):202–11.
[31] Krul SP, Berger WR, Smit NW, et al. Atrial fibrosis and conduction slowing in the left atrial appendage of patients undergoing thoracoscopic surgical pulmonary vein isolation for atrial fibrillation. Circ Arrhythm Electrophysiol 2015;8(2):288–95.
[32] Wu TJ, Ong JJ, Hwang C, et al. Characteristics of wave fronts during ventricular fibrillation in human hearts with dilated cardiomyopathy: role of increased fibrosis in the generation of reentry. J Am Coll Cardiol 1998;32(1):187–96.
[33] Andrade J, Khairy P, Dobrev D, Nattel S. The clinical profile and pathophysiology of atrial fibrillation: relationships among clinical features, epidemiology, and mechanisms. Circ Res 2014;114(9):1453–68.
[34] McDowell KS, Vadakkumpadan F, Blake R, et al. Mechanistic inquiry into the role of tissue remodeling in fibrotic lesions in human atrial fibrillation. Biophys J 2013;104(12):2764–73.
[35] Carrick RT, Benson B, Habel N, Bates OR, Bates JH, Spector PS. Ablation of multiwavelet re-entry guided by circuit-density and distribution: maximizing the probability of circuit annihilation. Circ Arrhythm Electrophysiol 2013;6(6):1229–35.
[36] Spector PS, de Sa DDC, Tischler ES, et al. Ablation of multi-wavelet re-entry: general principles and in silico analyses. Europace 2012;14(Suppl. 5):v106–11.
[37] Cao X, Aimoto M, Fukumoto M, Nagasawa Y, Tanaka H, Takahara A. Influence of chronic volume overload-induced atrial remodeling on electrophysiological responses to cholinergic receptor stimulation in the isolated rat atria. J Pharmacol Sci 2018;136(2):73–8.
[38] Chen YJ, Chen SA, Tai CT, et al. Electrophysiologic characteristics of a dilated atrium in patients with paroxysmal atrial fibrillation and atrial flutter. J Interv Card Electrophysiol 1998;2(2):181–6.
[39] Wijffels MC, Kirchhof CJ, Dorland R, Power J, Allessie MA. Electrical remodeling due to atrial fibrillation in chronically instrumented conscious goats: roles of neurohumoral changes, ischemia, atrial stretch, and high rate of electrical activation. Circulation 1997;96(10):3710–20.
[40] Ravelli F, Allessie M. Effects of atrial dilatation on refractory period and vulnerability to atrial fibrillation in the isolated Langendorff-perfused rabbit heart. Circulation 1997;96(5):1686–95.
[41] Bode F, Katchman A, Woosley RL, Franz MR. Gadolinium decreases stretch-induced vulnerability to atrial fibrillation. Circulation 2000;101(18):2200–5.
[42] Oliveira M, da Silva MN, Timoteo AT, et al. Inducibility of atrial fibrillation during electrophysiologic evaluation is associated with increased dispersion of atrial refractoriness. Int J Cardiol 2009;136(2):130–5.
[43] Soylu M, Demir AD, Ozdemir O, et al. Increased dispersion of refractoriness in patients with atrial fibrillation in the early postoperative period after coronary artery bypass grafting. J Cardiovasc Electrophysiol 2003;14(1):28–31.
[44] Zhang Y, Wang YT, Shan ZL, Guo HY, Guan Y, Yuan HT. Role of inflammation in the initiation and maintenance of atrial fibrillation and the protective effect of atorvastatin in a goat model of aseptic pericarditis. Mol Med Rep 2015;11(4):2615–23.
[45] Yu L, Li X, Huang B, et al. Atrial fibrillation in acute obstructive sleep apnea: autonomic nervous mechanism and modulation. J Am Heart Assoc 2017;6(9).
[46] Ellinwood N, Dobrev D, Morotti S, Grandi E. In silico assessment of efficacy and safety of IKur inhibitors in chronic atrial fibrillation: role of kinetics and state-dependence of drug binding. Front Pharmacol 2017;8:799.
[47] Baumgartner H, Falk V, Bax JJ, De Bonis M, Hamm C, Holm PJ, et al. ESC/EACTS guidelines for the management of valvular heart disease: the task force for the Management of Valvular Heart Disease of the European Society of Cardiology (ESC) and the European Association for Cardio-Thoracic Surgery (EACTS). Eur Heart J 2017: 2017.
[48] Kottkamp H, Bender R, Berg J. Catheter ablation of atrial fibrillation: how to modify the substrate. J Am Coll Cardiol 2015;65:196–206.
[49] Krämer J, Niemann M, Liu D, et al. Two-dimensional speckle tracking as a non-invasive tool for identification of myocardial fibrosis in Fabry disease. Eur Heart J 2013;34(21):1587–96.
[50] Ambale-Venkatesh B, Lima JA. Cardiac MRI: a central prognostic tool in myocardial fibrosis. Nat Rev Cardiol 2015;12(1):18–29.
[51] Levy F, Rusinaru D, Maréchaux S, Charles V, Peltier M, Tribouilloy C. Determinants and prognosis of atrial fibrillation in patients with aortic stenosis. Am J Cardiol 2015;116:1541–6.
[52] Thihalolipavan S, Morin DP. Atrial fibrillation and heart failure: update 2015. Prog Cardiovasc Dis 2015;58:126–35.
[53] Pourafkari L, Ghaffari S, Bancroft GR, Tajlil A, Nader ND. Factors associated with atrial fibrillation in rheumatic mitral stenosis. Asian Cardiovasc Thorac Ann 2015;23: 17–23.
[54] Nakatani Y, Nishida K, Sakabe M, Kataoka N, Sakamoto T, Yamaguchi Y, et al. Tranilast prevents atrial remodeling and development of atrial fibrillation in a canine model of atrial tachycardia and left ventricular dysfunction. J Am Coll Cardiol 2013;61:582–8.
[55] He Z, Sun C, Xu Y, Cheng D. Reduction of atrial fibrillation by Tanshinone IIA in chronic heart failure. Biomed Pharmacother 2016;84:1760–7.
[56] Dosdall DJ, Ranjan R, Higuchi K, Kholmovski E, Angel N, Li L, et al. Chronic atrial fibrillation causes left ventricular dysfunction in dogs but not goats: experience with dogs, goats, and pigs. Am J Physiol Heart Circ Physiol 2013;305:H725–31.